Crystal structure of pseudo-six-fold carbon dioxide phase II at high pressures and temperatures

C. S. Yoo,[1,*] H. Kohlmann,[2] H. Cynn,[1] M. F. Nicol,[2] V. Iota,[1] and T. LeBihan[3]
[1]*Lawrence Livermore National Laboratory, University of California, Livermore, California 94551*
[2]*High Pressure Science and Engineering Center and Departments of Physics and Chemistry, University of Nevada Las Vegas, Las Vegas, Nevada 89154-4002*
[3]*European Synchrotron Radiational Facility, Grenoble, France*
(Received 29 November 2001; published 12 February 2002)

The crystal structure of CO_2-II is determined to be tetragonal $P4_2/mnm$ with $z=2$, with evidence of some tetragonal-to-orthorhombic (*Pnnm*) disorder in the *ab* plane. In this structure, carbon atoms are pseudo-sixfold-coordinated by oxygens; two oxygens are at an elongated intramolecular C═O bond distance, 1.331(3) Å, and four are at a collapsed intermolecular distance, 2.377(2) Å, at the apices of highly distorted octahedral. Strong intermolecular association results in a large splitting of the symmetric stretching ν_1 mode and in a high bulk modulus 131.5 GPa. At 11 GPa, CO_2-II is about 6.8% denser than CO_2-III (*Cmca*).

DOI: 10.1103/PhysRevB.65.104103 PACS number(s): 64.70.Kb, 81.30.−t

INTRODUCTION

A fundamental principle of high-pressure chemistry is that multiple bonds become unstable because a rapid increase of electron kinetic energies overtakes locally attractive electrostatic potential energies for valence electrons. This instability delocalizes electrons confined within intramolecular bonds, and eventually transforms molecular solids to monoatomic metallic phases at high pressure.[1] Such insulator-to-metal transitions typically occur well above 100 GPa in simple molecular solids. However, theoretical calculations[2,3] predict that, even at intermediate pressures far lower than the insulator-to-metal transition pressures, molecular solids may transform into nonmolecular framework structures. The recent discoveries of polymeric carbon dioxide[4] and nitrogen[5] indeed prove this proposal. Importantly, these nonmolecular solids exhibit very interesting physical properties such as optical nonlinearity,[4] low compressibility,[6] high-energy density,[7] and semiconductivity,[8] and thus offer great promises for future development of novel interesting materials.

Large differences exist between molecular and nonmolecular phases in the nature of bonding, intermolecular interactions, molecular configurations, crystal structures, and electronic structures. Therefore, molecular-to-nonmolecular phase transitions may follow very complicated pathways whose explanations present fundamental scientific challenges in condensed-matter physics. The phase diagram of carbon dioxide is a good example of the complexity of phases and transitions. Carbon dioxide at high pressure and temperature occurs in many polymorphs of greatly different chemical bonding and intermolecular interactions.[9] A very unusual, strong intermolecular association evident in the large splitting of the ν_1 vibration, without accompanying evidence of intermolecular bonding such as the ν_1(C-O-C) vibration observed in polymeric CO_2-V[4] makes phase II of CO_2 of particular interest. More importantly, the stability field of phase II is in a pressure-temperature region between the stability regions of the molecular and nonmolecular phases, suggesting that phase II is a key to understanding the molecular-to-nonmolecular phase transition.

In this study we characterize the crystal structure of CO_2-II *in situ* at high pressures and temperatures. The results show evidence of a strong molecular association of phase II in the configuration of pseudo-six-fold carbon atoms in a structure similar to SiO_2 stishovite.[10] Based on its elongated intramolecular bond distance, well over 1.30 Å, and collapsed intermolecular distance, below 2.38 Å, we conclude that CO_2-II is intermediate between molecular and nonmolecular solids.

EXPERIMENTS

Carbon dioxide samples were prepared by condensing CO_2 gas at −40 °C and 10 atm into diamond-anvil cells contained in a pressure vessel. The CO_2-I was warmed to ambient temperature, and compressed until it transformed to CO_2-III, above 11 GPa. Phase II was then synthesized by externally heating the phase-III sample to above the III-to-II transition temperatures at pressures between 11 and 50 GPa.[9] The sample temperature was measured with a precision of ~1 K by using a calibrated thermocouple (*K* type) in contact with the anvils. A few micron-sized ruby crystals were loaded in the cell to determine pressures.[11] Phase II was readily recognized both by its highly polycrystalline visual appearance and its characteristic Raman spectrum.[9] We often observed a large pressure drop, nearly 10%, after the III-to-II transition.

The crystal structure of CO_2-II was determined *in situ* at high pressures and temperatures by angle-resolved x-ray diffraction (ADXD) using a focused monochromatic synchrotron x ray at ID-30 of the European Synchrotron Radiation Facility ($\lambda = 0.3738$ Å) and at BL 10-2 of Stanford Synchrotron Radiation Laboratory ($\lambda = 0.6199$ Å). The diffraction patterns were recorded on high-resolution image plates, and were analyzed by using the FIT2D program.[12] The ADXD powder patterns were then Rietveld refined by using FULLPROF98 (Ref. 13) and RIQAS.[14]

RESULTS AND DISCUSSION

Figure 1 shows a typical powder x-ray diffraction pattern of CO_2-II at 28 GPa and 680 K. The diffraction pattern can be indexed to tetragonal or pseudotetragonal unit cells. Based on the systematic absence of diffraction lines ob-

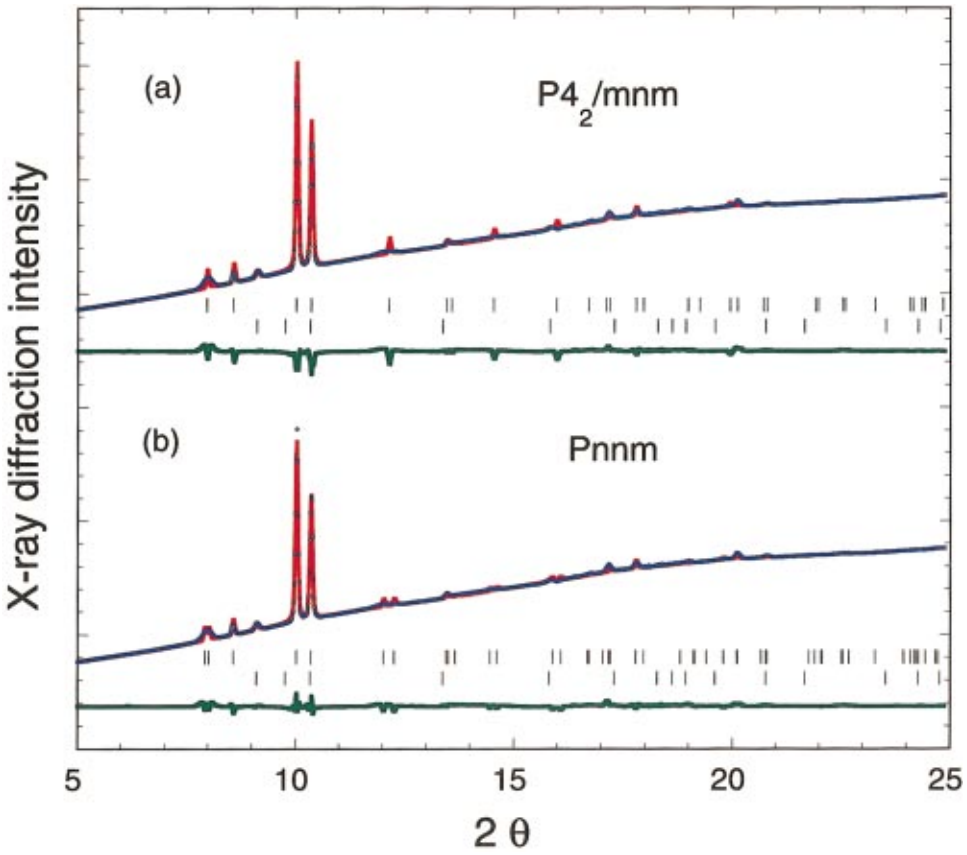

FIG. 1. (Color) Observed (circles), calculated (solid line), and difference (bottom) x-ray-diffraction pattern of CO_2-II at 28 GPa and 680 K, assuming (a) a tetragonal model and (b) an orthorhombic model. The Bragg markers denote reflection positions of CO_2-II (top) and rhenium (gasket material, bottom). Note that the 101 and 200 reflections are relatively broad as a result of the tetragonal-to-orthorhombic disorder in the *ab* plane to the $CaCl_2$ (*Pnnm*) structure. Residual factors for the refinements are (a) $R_{wp}=0.205$, $R_{Bragg}=0.269$, (b) $R_{wp}=0.122$, $R_{Bragg}=0.172$. Note that background-corrected intensities y_i(obs) have been used for the calculation, resulting in relatively high R_{wp} factors. Definition of R factors: $R_{wp}=\{\Sigma w_i[y_i(\text{obs})-y_i(\text{calc})]^2/\Sigma w_i y_i(\text{obs})^2\}^{1/2}$; $R_{Bragg}=\Sigma|I_B(\text{obs})-I_B(\text{calc})|/\Sigma I_B(\text{obs})$.

served, we conclude that two space groups are possible: a rutilelike tetragonal cell (the space group $P4_2/mnm$) and a $CaCl_2$-like orthorhombic cell ($Pnnm$), which represents only a minor modification of the tetragonal cell. For the structure refinements the background was described by interpolation between 22 points, and the pseudo-Voigt function was used for modeling reflection profiles. (a) For the $P4_2/mnm$ model, a total of 12 parameters was refined for CO_2-II: one scale factor, one positional, two lattice, one mixing, two halfwidths, one preferred orientation (direction *c*), and one asymmetry parameter for CO_2-II and one scale factor, one lattice and one haldwidth for Re (gasket material). The initial lattice parameters of Re were estimated from the compression curve previously obtained,[15] and the c/a ratio was constrained to be 1.613. The Debye-Waller factors of carbon and oxygen held fixed at reasonable values. (b) For the *Pnnm* model, the refinement was performed as described above with the only difference being that, according to the lower symmetry two more structural parameters were included and the Debye-Waller factors of carbon and oxygen could be refined freely, resulting in a total of 16 refined parameters. The Debye-Waller factors B were found 5.9(4) Å^2 for carbon and 4.9(2) Å^2 for oxygen, using a form $T=\exp-B[(\sin\theta/\lambda)^2]$ for the temperature factor. An even better fit could be achieved by assuming a mixture of the orthorhombic and tetragonal phases; however, there is no indication that the sample is not in a single phase.

Assuming the $P4_2/mnm$ structure, the final refinement yields, for lattice parameters, $a=b=3.5345(7)$ Å and $c=4.1401(7)$ Å, and for atomic positions, $C(2a)$ on (0,0,0) and $O(4f)$ on [0.2732(2),0.2732(2),0]. The final refined x-ray-diffraction pattern shows a reasonable agreement with the measured one with the exceptions on two broad (101) and (200) reflections at $2\theta=7.98°$ and 12.05°, respectively (Fig. 1). The orthorhombic space group, on the other hand, splits those two broad reflections and results in a somewhat better fit. For this space group, the final lattice parameters were $a=3.4883(7)$ Å, $b=3.5698(8)$ Å, and $c=4.1466(5)$ Å with atoms located at $C(2a)$ (0,0,0) and $O(4g)$ [0.2658(9),0.2667(9),0.0]. That is, the orthorhombic (*Pnnm*) cell represents only a slight, ~1%, distortion of the *ab* plane, and virtually the same *c* axis from the tetragonal ($P4_2/mnm$) structure. The calculated bond lengths and intermolecular distances are very similar in both models.

The crystal structure of CO_2-II lattice can be described as

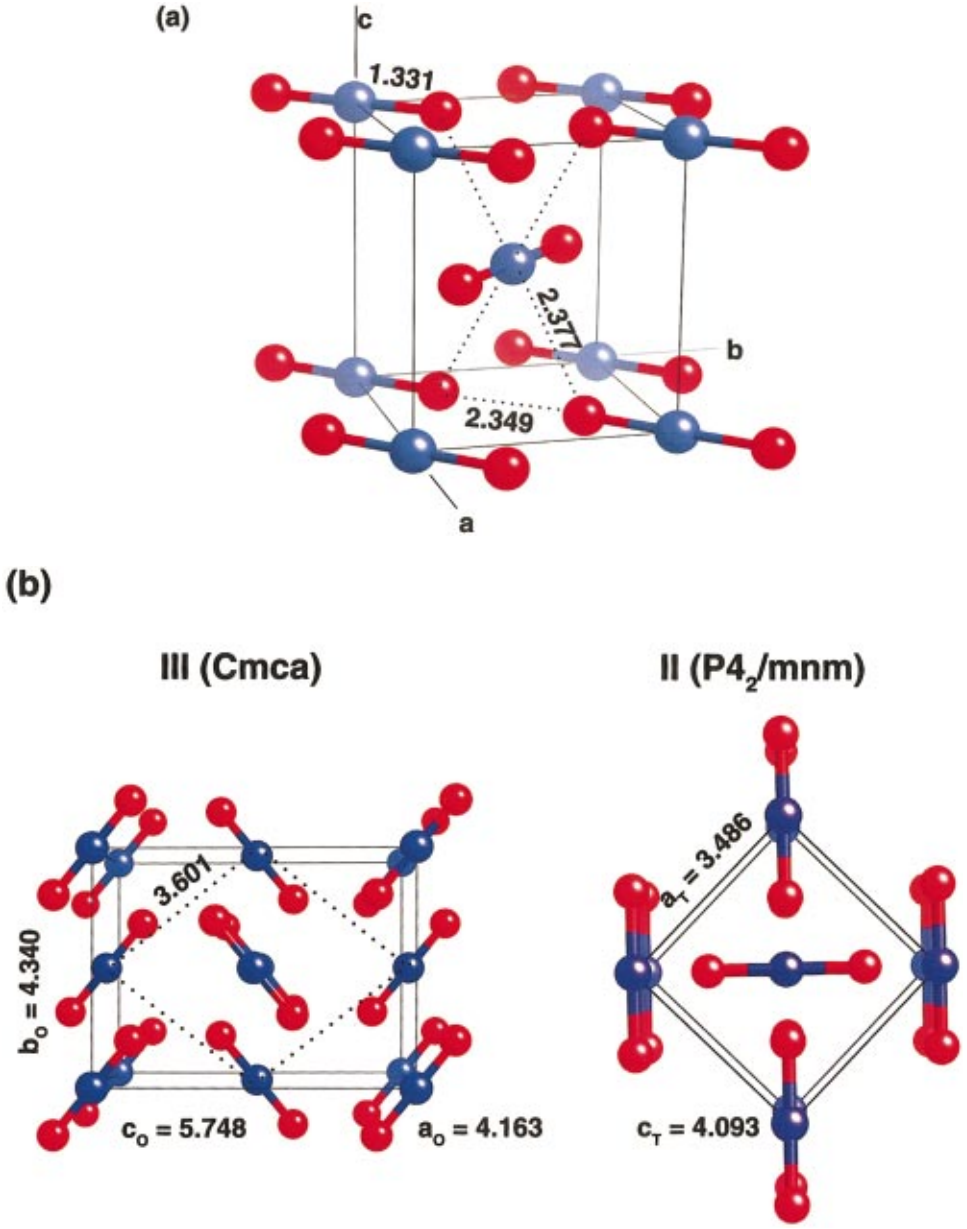

FIG. 2. (Color) (a) Crystal structure of CO_2-II at 28 GPa and 680 K. Note that six oxygen atoms neighbor each carbon atom at the apices of an elongated pseudo-octahedron. Each oxygen atom is, on the other hand, threefold coordinated with carbon atoms. Also, note the very close nonbonded O···O distance along [110], causing the dynamic disorder in the lattice. This structure is analogous to the stishovite structure of SiO_2. (b) The unit cells of CO_2-III (*Cmca*, $Z=4$, left; projected along the *a* axis) and CO_2-II ($P4_2/mnm$, $Z=2$, right; projected along the *c* axis) are compared to show their close structural relationship at 30 GPa and ambient temperature: $a_T=b_T=1/2\ (a_O^2+b_O^2)^{1/2}$ and $c_T=a_O$, where the subscripts *O* and *T* depict the orthorhombic phase III and tetragonal phase II structures, respectively. All numbers in the figure are in Å.

a sixfold layer structure similar to rutile and SiO_2-stishovite (both in $P4_2/mnm$) or $CaCl_2$ (*Pnnm*) (Fig. 2). All CO_2 molecules are arranged in layers perpendicular to crystallographic *c* axis; half at $z=0$ with the molecular axis aligned along the face diagonal [110] direction, and the other half at $z=0.5$ aligned along the [−110] direction. In this configuration, each carbon atom has six neighboring oxygen atoms at the apices of highly distorted octahedral: two bonded oxygens at the distance 1.331(3) Å and four nonbonded ones at 2.377(2) Å. Each oxygen atom, on the other hand, has three nearest carbon atoms: one bonded and two nonbonded. Note that the carbon-oxygen bond is highly elongated from a typical C═O double bond distance (<1.2 Å); whereas the nearest intermolecular distance is nearly collapsed to substantially less than twice the C—O bond distance. In these respects, this structure clearly represents a strong association of neighboring molecules, and can be considered as an intermediate state between a molecular crystal and an extended solid like rutile or SiO_2 stishovite.

Recall that the (101) and (200) reflections in Fig. 1 are not

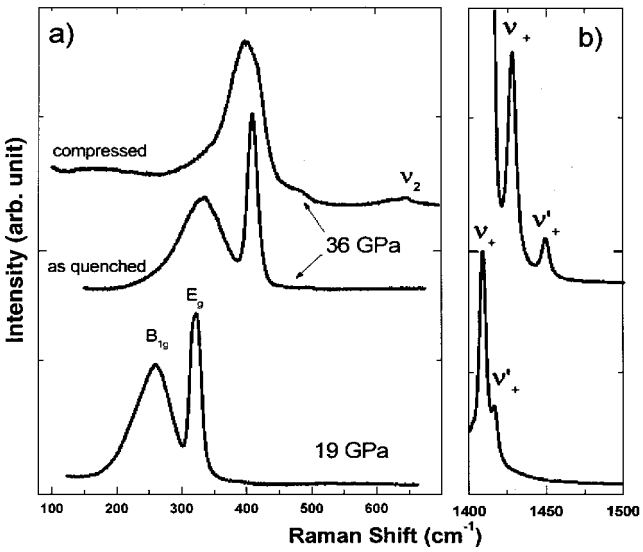

FIG. 3. Raman spectra of CO_2-II at high temperatures and pressures. (a) Low-frequency modes: The low frequency B_{1g} shearlike libration is extremely broad due to oscillatory motions of oxygen atoms, resulting in a dynamic tetragonal-to-orthorhombic lattice distortion in the *ab* plane. Note that the sharp E_g band splits into two and the bending ν_2 mode appears, upon compression of the quenched phase II at ambient temperature (marked as ''compressed''). This sample was initially quenched at 19 GPa and then compressed to 36 GPa at ambient temperature. The sharp difference of the B_{1g} modes between the ''as quenched'' and ''compressed'' samples at 36 GPa indicates the high sensitivity of nonbonded O···O interaction to lattice strain. (b) High-frequency mode: The large splitting of the Fermi resonance band into the ν_+ and ν'_+ (or ν_1-A_{1g} and ν'_1-B_{2g}) modes implies strong association of CO_2 molecules in this phase II. Such a large splitting of the ν_+ mode is absent in the other phases of CO_2-I, -III, and -IV (Ref. 9).

well resolved, but are very broad even at high temperatures at relatively low pressures. It is well known that, for rutile and rutilelike oxides,[16] a minor stress anisotropy distorts the rutile structure ($P4_2/mnm$) into a calcium chloride structure (*Pnnm*). Such a distortion is especially important for any crystallite aligned so that its *c* axis makes any nonzero angle to the symmetry axis of the diamond-anvil cell. For a randomly aligned powder, the orientations and range of distortions would show dispersion, thereby broadening some diffraction bands like the (101) and (200) bands. The very short interatomic distance, 2.349 Å, between nonbonded O···O along the [110] directions may even cause the oxygen atoms to oscillate, thereby dynamically disordering the structure in the *ab* plane and broadening the reflections (Fig. 1).

The Raman spectrum of CO_2-II (Fig. 3) is also in support of the strong molecular association and dynamic disorder in CO_2-II. The irreducible representation of the Raman-active vibrations of rutile or stishovite [the $P4_2/mnm$ (D_{4h}^{14}) structure with $Z=2$] can be written as $\Gamma_{\text{Raman}}=A_{1g}+B_{1g}+B_{2g}+E_g$.[17] Following this assignment for the CO_2-II phase, A_{1g} and B_{2g} become equivalent to the internal stretching vibration modes, in phase (ν_1) and out of phase (ν_1), respectively. B_{1g} and E_g represent the external vibration modes: a shear-type libration in the *ab* plane and a rocking motion along the *c* axis, respectively. The very low frequency of the broad B_{1g} vibration mode in Fig. 3(a) is consistent with the concept of the dynamic disorder of the lattice. Furthermore, the B_{1g} mode nearly disappears upon compression [the spectrum marked as ''compressed'' in Fig. 3(a)], which reflects the high sensitivity of nonbonded O···O interaction to the lattice strain. The large splitting of the ν_1 mode (or its Fermi resonance branch ν_+) in Fig. 3(b) also suggests the strong association of molecules.

The pressure-volume curve of CO_2-II (Fig. 4) illustrates a highly unusual molecular behavior nearly resembling the behavior of an extended phase. Note that CO_2-II is substantially denser than CO_2-III by 9.6% at ambient pressure. The large volume collapse associated with the III-to-II transition (by about 7–5 % between 11 and 50 GPa) is also consistent with the large pressure drop observed after the transition occurs. The third order Birch-Murnaghan equation-of-state fit to the pressure-volume data (solid line) yields the bulk modulus $B=131$ GPa (its pressure derivative is $B'=2.1$) for CO_2-II, even greater than that of CO_2-III, 87 GPa ($B'=3.3$).[8] Remember that phase III already supports an unusually large lattice strain for a molecular solid, especially above 20 GPa.[6] For comparison, the bulk modulus of the phase I is 6.2 GPa ($B'=6.1$), typical for a molecular phase. Table I summarizes the unusual compressibilities of CO_2 phases in comparison with those of other typical covalent solids, metals, and molecular solids.

Note that CO_2-I transforms into CO_2-III rather than more energetically favorable CO_2-II at ambient temperature.[9,18] This result can be interpreted as the following. The transition from phase I to phase II is diffusion limited, because of a

TABLE I. The equation-of-state parameters for CO_2 phases in comparison with those of other solids. The third-order Birch-Murnaghan equation of state was used to fit the data and obtain the compressibility (B_o), its pressure derivative (B'), and the density ρ_o.

Solids	ρ (g/cm^3)	B_o (GPa)	B'	References
Covalently bonded solids				
Diamond	3.51	444	1.9	25
Cubic-BN	3.48	369	4.5	26
CO_2-*V*	2.90	365	0.8	this study
SiO_2 stishovite	4.29	313	1.7	27
Al_2O_3 ruby	3.98	239	0.9	28
Metals and semiconductors				
hcp-Fe	8.30	165	5.3	29
CO_2-II	2.45	131	2.1	this study
Silicon	2.33	98	4.2	30
CO_2-III	2.22	87	3.3	this study
Al	2.70	72	5.3	31
Molecular solids				
CO_2-I	1.75	6	6.1	this study
δ-N_2	1.03	3	3.9	32
fcc-Xe	3.46	4	5.5	33

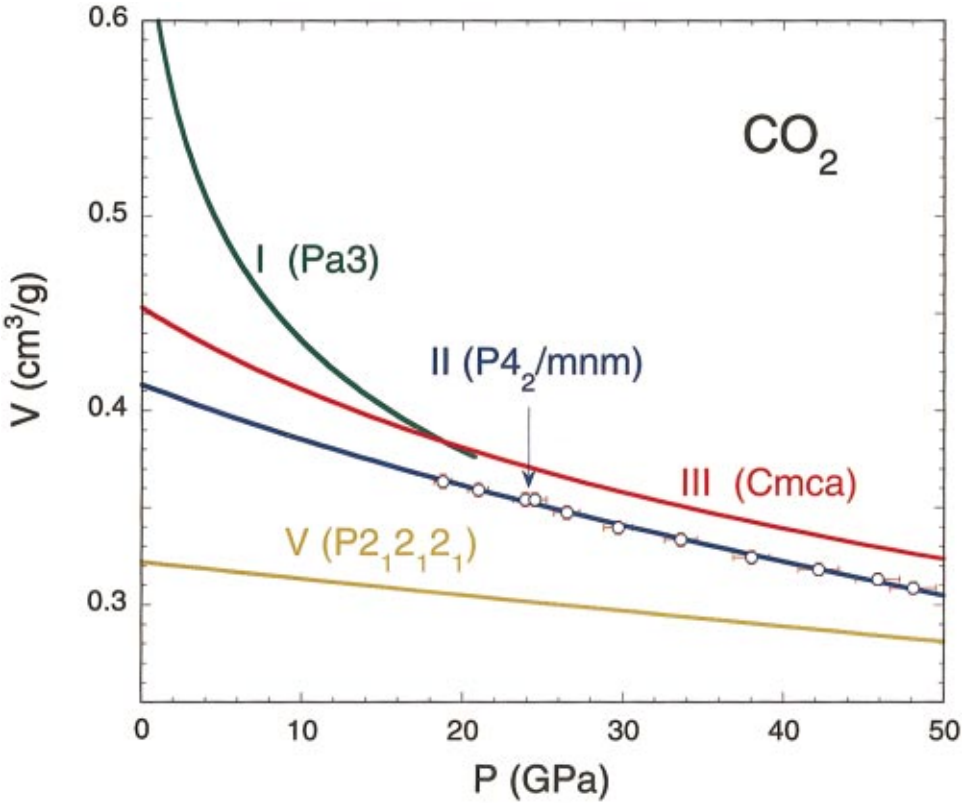

FIG. 4. (Color) The pressure-volume isotherm of CO_2-II compared with those of CO_2-I, CO_2-III, and CO_2-V at 300 K. A Birch-Murnaghan equation-of-state fit to the CO_2-II data (the blue line) yields a high bulk modulus $B_o = 131.5$ GPa and a relatively low pressure derivative $B' = 2.1$. The large B_o and crystal structure (Fig. 1) indicate that the phase II is highly unusual for a molecular phase and should be considered as an intermediate phase between molecular and extended solids. Note a relatively large difference volume change associated with the III-to-II phase transition, ~5–7 % depending on pressure.

large volume difference between the two phases (~12.3% at 11 GPa in Fig. 4), and the reconstructive nature of the transition. In contrast, the transition from phase I to phase III requires only a minor modification of the lattice, mainly the rotation of CO_2 molecules,[19] which occurs martensitically under the presence of a small lattice strain. In addition, because of the close structural relationship between the phases III and II [Fig. 2(b)], the III-to-II transition can occur without a large transition barrier despite the phases relatively large volume difference. Thus the transition from molecular phase I to pseudo-six-fold phase II favors the mechanism via metastable phase III. The presence of such a ''precursor'' phase III transforming into a stable rutilelike phase II in CO_2 is somewhat analogous to anatase transforming into rutile in TiO_2.[20]

SUMMARY

In this study, we have characterized the crystal structure of CO_2-II ($P4_2/mnm$), and discussed tetragonal-to-orthorhombic (*Pnnm*, $CaCl_2$-like) distortion and the dynamic disorder which likely occurs in this structure because of a short O···O distance, 2.35 Å, in the *ab* plane. The refined x-ray data indicate that carbon atoms in CO_2-II are pseudo-six-fold coordinated with oxygen atoms, whereas oxygen atoms are threefold coordinated with carbon atoms. Based on its elongated intramolecular bond distance, well over 1.30 Å, and collapsed intermolecular distance, below 2.38 Å, we conclude that CO_2-II is an intermediate between molecular and nonmolecular solids. Strong intermolecular association of CO_2 molecules in this highly distorted octahedral configuration results in a high bulk modulus 131 GPa and in a large splitting of the symmetric stretching ν_1 mode as observed in the Raman spectrum.

The crystal structure and properties of CO_2-II clearly exhibit characteristics of a quasi-extended phase, similar to that of SiO_2 stishovite. However, CO_2-II is different from stishovite in three ways: (1) because of high covalency in C—O bonds,[6,21,22] the O-C-O and O-C-O angles are more rigid and favor 110°–130°, which contrasts with a wider range of angles, 90°–180°, observed in various SiO_2 polymorphs.[23,24] (2) There are no nearby *d* bands in carbon, which makes it difficult to stabilize nonbonding electrons of oxygen atoms at pressures below 100 GPa. As a result, the transition of CO_2-II to a ''perfect'' sixfolded extended phase is limited at these intermediate pressures. Instead, the lattice develops various distortions like a tetragonal-to-orthorhombic distortion and a bending of linear molecules, which precede a transition to a fourfold carbon dioxide-*V* phase. (3) Finally, CO_2-II appears at lower pressures than four-fold CO_2-*V*, whereas sixfold stishovite appears at substantially higher pressures than fourfold quartz and coesite. Clearly, it reflects the intermediate nature of CO_2-II between molecular and extended solids.

ACKNOWLEDGMENTS

The x-ray diffraction in this study was done at the ESRF, and also in part at the SSRL. We appreciate K. Visbeck for assisting with the experiments. We also thank F. Gygi for very productive numerous discussions and for sharing his unpublished results. This work was supported by the LDRD and PDRP programs of the LLNL, University of California, under the auspices of the U.S. Department of Energy under Contract No. W-7405-ENG-48.

*Email address: yoo1@llnl.gov

[1] S. Desgreniers, Y. K. Vohra, and A. L. Ruoff, J. Phys. Chem. **94**, 1117 (1990).
[2] A. K. McMahan and R. LeSar, Phys. Rev. Lett. **54**, 1929 (1985).
[3] C. Mailhiot, L. H. Yang, and A. K. McMahan, Phys. Rev. B **46**, 14 419 (1992).
[4] V. Iota, C. S. Yoo, and H. Cynn, Science **283**, 1510 (1998).
[5] A. F. Goncharov, E. Gregoryanz, H. K. Mao, Z. Liu, and R. J. Hemley, Phys. Rev. Lett. **85**, 1262 (2000).
[6] C. S. Yoo, H. Cynn, F. Gygi, G. Galli, V. Iota, M. Nicol, S. Carlson, D. Hauserman, and C. Mailhiot, Phys. Rev. Lett. **83**, 5527 (1999).
[7] K. O. Kristie, W. W. Wilson, J. A. Shirley, and J. A. Boatz, Angew. Chem. Int. Ed. Engl. **38**, 2002 (1999).
[8] M. L. Erements, R. J. Russell, H. K. Mao, and E. Gregoryanz, Nature (London) **411**, 170 (2001).
[9] V. Iota and C. S. Yoo, Phys. Rev. Lett. **86**, 5922 (2001).
[10] S. M. Stishov and N. V. Belov, Dokl. Akad. Nauk SSSR **143**, 951 (1962); W. Sinclair and A. E. Ringwood, Nature (London) **272**, 714 (1978).
[11] J. Yen, Ph.D. thesis, UCLA, 1986.
[12] A. P. Hammersley, *FIT2D V9.129 Reference manual v3.1*, ESRF Report No. 98HA01T, 1998 (unpublished)
[13] J. Rodriguez-Carvajal, FullProf. 98, LLB (1998).
[14] Q. Johnson, Riquas© (1999) (MDI, California).
[15] R. Rao and A. Rammanand, J. Phys. Chem. Solids **39**, 145 (1978).
[16] M. Nicol and M. Y. Fong, J. Chem. Phys. **54**, 3167 (1971); J. F. Mammone, M. Nicol, and S. K. Sharma, J. Phys. Chem. Solids **42**, 379 (1981).
[17] R. J. Hemley, H. K. Mao, and E. C. T. Chao, Phys. Chem. Miner. **13**, 285 (1986).
[18] F. Gygi (unpublished).
[19] K. Aoki, H. Yamawaki, M. Sakashita, T. Gotoh, and K. Takemura, Science **263**, 356 (1994).
[20] L. Nagel and M. O'Keeffe, Mater. Res. Bull. **6**, 1317 (1971).
[21] B. Holm, R. Ahuja, A. Belomoshko, and B. Johansson, Phys. Rev. Lett. **85**, 1258 (2000).
[22] J. Dong, J. K. Tomfohr, and O. F. Sankey, Phys. Rev. B **61**, 5967 (2000).
[23] R. M. Hazen, L. W. Finger, R. J. Hemley, and H. K. Mao, Solid State Commun. **72**, 507 (1989).
[24] H. Gratsch and O. W. Flörke, Z. Kristallogr. **195**, 31 (1991).
[25] I. V. Alexandrov *et al.*, Sov. Phys. JETP **66**, 384 (1987).
[26] E. Knittle *et al.*, Nature (London) **337**, 349 (1989).
[27] N. L. Russ *et al.*, Am. Mineral. **75**, 739 (1990).
[28] Y. Sato and S. Akimoto, J. Appl. Phys. **50**, 5285 (1978).
[29] E. Huang, W. A. Bassett, and P. Tao, J. Geophys. Res. **92**, 8129 (1987).
[30] I. L. Spain *et al.*, High Temp.-High Press. **16**, 507 (1983).
[31] L. C. Ming *et al.*, Physica **139 & 140B**, 174 (1986).
[32] H. Olijnyk, J. Chem. Phys. **93**, 8968 (1990).
[33] H. Cynn *et al.*, Phys. Rev. Lett. **86**, 4552 (2001).